



# Mg–Al hydrotalcites as efficient catalysts for aza-Michael addition reaction: A green protocol

Mohamed Mokhtar<sup>a,b,\*</sup>, Tamer S. Saleh<sup>a,c</sup>, Sulaiman N. Basahel<sup>a</sup>

<sup>a</sup> Chemistry Department, Faculty of Science, King Abdulaziz University, Jeddah 21533, Saudi Arabia

<sup>b</sup> Physical Chemistry Department, National Research Centre, Dokki, Cairo 12622, Egypt

<sup>c</sup> Green Chemistry Department, National Research Centre, Dokki, Cairo 12622, Egypt

## ARTICLE INFO

### Article history:

Received 22 September 2011

Received in revised form

12 November 2011

Accepted 13 November 2011

Available online 23 November 2011

### Keywords:

Mg–Al-hydrotalcite

Aza-Michael addition

Green protocol

Acidic/basic sites

Pyrazolo[1,5-*a*]pyrimidine

Microwave irradiations

## ABSTRACT

Mg–Al hydrotalcite was synthesized by a co-precipitation method. We have studied the effect of calcination temperature and hydration of the calcined phases on their catalytic activity for the synthesis of pyrazolo[1,5-*a*]pyrimidine derivatives (aza-Michael addition product). The structure of the as-synthesized sample and the presence of the anions in the interlayer galleries of hydrotalcites, have been determined by X-ray diffraction and FTIR spectroscopy. On calcining the material at 450 °C, it was amorphous periclase phase. Re-hydration of the calcined phase resulted in the formation of hydrotalcite-like phase. Such treatment to the as-synthesized hydrotalcite significantly changed the pore structure and the BET-surface area as determined from N<sub>2</sub> physisorption at 77 K. The as-synthesized Mg–Al-hydrotalcite catalyst was found to be the most efficient for the aza-Michael reaction relative to the activated solid catalysts tested. The high performance of this catalyst was attributed to the co-operative contribution of its acidic and basic sites. We have shown that this microwave assisted reaction provides an eco-friendly alternative to the conventional syntheses where soluble bases are used. Furthermore, the reaction was performed over a considerably shorter time scale and generated significantly higher yields than traditional methods.

© 2011 Elsevier B.V. All rights reserved.

## 1. Introduction

Many organic syntheses of fine chemicals use homogenous catalysts like minerals or organic acids and bases. The uses of such homogenous catalysts can be problematic since it can be difficult to recover the catalyst, a large quantity of waste is produced, and pipes can be corroded due to the salts used. A “green” alternative for these reactions that has high yields and good selectivity, along with a reduction in waste, can be carried out using solid acidic and basic catalysts. Such solid catalysts provide benign processes, with easier catalyst recovery procedures, and safer and easier operation modes. Furthermore, they do not need a polar solvent and the reaction can be conducted at higher temperatures or in vapor phase under heterogeneous conditions [1].

Layered double hydroxides [LDHs], generally named hydrotalcites, and thermally activated LDH products are useful catalysts, catalyst precursors and catalyst support materials for a broad range of organic reactions [2–5]. The structure of LDH can be visualized

as the structure of brucite, Mg(OH)<sub>2</sub>, in which some of the Mg<sup>2+</sup> cations, coordinated octahedrally by hydroxyl groups, are substituted by trivalent ions such as Al<sup>3+</sup>. The excess of positive charges in the LDH layers is compensated by anions and water, located in the interlayer spaces. The surface properties of the minerals can be tailored with relative ease by variation of the cations in the octahedral sheet during synthesis and by introducing different compensating anions in the interlayer regions. A whole class of catalytically active species can be made by performing a simple precipitation experiment, and it is worth noting that both the layered hydroxides of metal mixtures and mixed metal oxides (MMO), (the products obtained by thermal decomposition of LDH), are regarded as catalytically active. Thus, it is unsurprising that the syntheses of a variety of organic transformations including condensation, isomerization, anion exchangers and epoxidation reactions have been carried out using hydrotalcite catalysts [6–16].

Conjugate addition to  $\alpha,\beta$ -unsaturated carbonyl compounds (i.e. Michael addition) is one of the most important carbon–carbon and carbon–heteroatom bond-forming strategies for synthetic organic chemistry [17]. Common conjugate addition reactions involve the addition of a protic nucleophile donor (e.g., Si, Sn, N, P, O, S, Se, I, or H) to an alkene or alkyne acceptor that is activated by an electron-withdrawing group (e.g., ketone, ester, amide, nitrile, nitro, sulfonate, and phosphonate). Subsequently,

\* Corresponding author at: Chemistry Department, Faculty of Science, King Abdulaziz University, Jeddah 21533, Saudi Arabia. Tel.: +966 2 6194983; fax: +966 2 6952292.

E-mail address: [mmokhtar2000@yahoo.com](mailto:mmokhtar2000@yahoo.com) (M. Mokhtar).

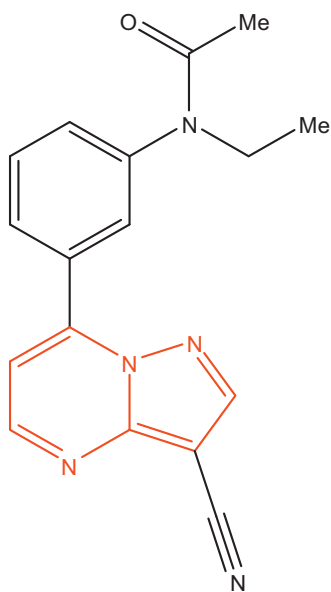


Fig. 1. Structure of Zaleplon.

the resulting incipient enolate is trapped with a proton source. There are a myriad of reported methodologies where successful Michael addition involves the use of base, these include piperidine in ethanol under reflux for 8 h [18], pyridine under reflux for 4 h [19], or addition of drops of piperidine under microwave irradiation [20]. However, these methodologies have one or more disadvantages, which include the use of high boiling and hazardous solvents, and the yields of the reactions tend not to be more than 70%. Aza-Michael additions have also been catalyzed using strong acids, but some side reactions occur, therefore some researchers have been working on the development of more mild catalytic systems for such aza-conjugation reactions. A number of alternative methodologies using Lewis acid catalysts have been reported, such as  $\text{PtCl}_4 \cdot 5\text{H}_2\text{O}$  [21],  $\text{Cu}(\text{OTf})_2$  [22],  $\text{InCl}_3$  [23],  $\text{Yb}(\text{OTf})_3$  [24,25],  $\text{LiClO}_4$  [26],  $\text{Bi}(\text{NO}_3)_3$  [27],  $\text{FeCl}_3 \cdot 6\text{H}_2\text{O}$  [28],  $\text{CeCl}_3 \cdot 7\text{H}_2\text{O}$  [29],  $\text{ZnO}$  [30],  $\text{Y}(\text{NO}_3)_3 \cdot 6\text{H}_2\text{O}$  assisted under solvent free condition [31], silica supported perchloric acid [32] and sulfated zirconia [33]. However, similar to the basic catalysts, many of the above methods suffer from some drawbacks, for example the requirement for a large excess of reagents, often it is necessary to use toxic solvents such as 1,2-dichloroethane or acetonitrile, and some catalysts are substrate-selective. Moreover, most of the above methods are not successful with heterocyclic amines, which limit their application, and more importantly, some of them have not been used for aza-Michael reaction with  $\alpha,\beta$ -unsaturated ketones as Michael acceptors. To our knowledge, a little has been reported on reactivity of  $\alpha,\beta$ -unsaturated ketones and amines utilizing solid base catalysts [34] and suffer from relatively low yield and long reaction time.

The aza-Michael addition reaction between 5-aminopyrazole derivatives and enaminone is considered a precursor for synthesis of novel pyrazolo[1,5-*a*]pyrimidine derivatives [35]. The pyrazolo[1,5-*a*]pyrimidine moiety is a privileged class of pharmacophore, since compounds bearing this structural unit possess a broad spectrum of biological activities [36,37] and they have potent analgesic effects [38]. Also, there are some pyrazolo[1,5-*a*]pyrimidine derivatives considered as ideal non-benzodiazapine sedative/hypnotic drugs, for example Zaleplon [39], marketed as *Sonata*<sup>TM</sup> (*N*-(3-(3-cyanopyrazolo[1,5-*a*]pyrimidin-7-yl)phenyl)-*N*-ethylacetamide (**1**) (Fig. 1), which is used in the treatment of insomnia.

The development of an efficient and green protocol for aza-Michael addition of heterocyclic amines to  $\alpha,\beta$ -unsaturated ketones still remains a challenging task and is highly desirable, especially for the preparation of chemically important and biologically active complex molecules. Microwave-assisted chemistry provides a convenient platform to perform reactions very efficiently in the absence of any organic solvents, under so-called dry media conditions (solvent free condition). The advantages of using dry media conditions range from faster reaction rates with different selectivity to more economical conditions due to the absence of organic solvents [40]. In addition microwave irradiation gives remarkable rate enhancement, higher yields, greater selectivity and easier manipulation.

Motivated by the aforementioned findings, and our ongoing endeavors in the development of environmentally benign protocols for fine chemical synthesis [41,42], we report Mg–Al-hydrotalcite as solid catalyst, and its activated forms, for aza-Michael addition of aminopyrazoles to enaminone derivatives under solvent-free conditions using microwave irradiation.

## 2. Experimental

### 2.1. Materials and methods

#### 2.1.1. Materials

Magnesium nitrate ( $\text{Mg}(\text{NO}_3)_2 \cdot 6\text{H}_2\text{O}$ ; 98.9%), aluminum nitrate ( $\text{Al}(\text{NO}_3)_3 \cdot 9\text{H}_2\text{O}$ ; 99.1%), sodium carbonate ( $\text{Na}_2\text{CO}_3$ ; 99.9%) and sodium hydroxide ( $\text{NaOH}$ ; 99.9%) were purchased from BDH Ltd., for the synthesis of hydrotalcite samples. The deionized water was used during the synthesis. 3-(Dimethylamino)-1-phenylprop-2-en-1-one **1a** [43], 3-(dimethylamino)-1-(4-fluorophenyl)prop-2-en-1-one **1a** [44] and 5-amino-1*H*-pyrazole derivatives **2b,c** [45] were prepared according to the reported literature.

#### 2.1.2. Catalyst synthesis

The Mg–Al hydrotalcite sample with Mg/Al molar ratio equal to 2.0, was synthesized by a co-precipitation method at constant pH [46]. A solution of 1 M Mg/Al nitrates was added dropwise to a vigorously stirred solution of 1 M  $\text{Na}_2\text{CO}_3/\text{NaOH}$  in a glass reactor at room temperature and pH = 10. Finally, the sample was washed by re-suspension in distilled water with gentle stirring, followed by filtration. This washing/filtration step was repeated 5 times until the precipitate was free from sodium ions as confirmed by ICP analysis. The precipitate was then dried in air at 80 °C for 16 h. Three different catalysts were synthesized, characterized and tested, they were: as-synthesized (HT-As), calcined at 450 °C (HT-450), dehydrated at 450 °C then rehydrated, in pre-boiled liquid water under gentle stirring for 1 h at 25 °C (HT-450-H).

### 2.2. Characterization of the catalysts

Elemental chemical analysis was performed using inductively coupled plasma-optical emission spectrometry (ICP-OES Plasma 400, Perkin Elmer, USA). Powder X-ray diffraction (XRD) patterns of hydrotalcites were recorded with powder diffractometer (Bruker, Advance-8 system) using  $\text{Cu K}\alpha$  radiation ( $\lambda = 1.54056 \text{ \AA}$ ) in the  $2\theta$  range from 2° to 80°. FTIR spectra were recorded in the range 550–4000  $\text{cm}^{-1}$  on Perkin Elmer Spectrum 100 FT-IR spectrometer. The infrared spectra were recorded at room temperature for the prepared products. The resulting FTIR spectral pattern was then analyzed and matched with known signatures of identified materials from the FTIR library.  $\text{N}_2$  physisorption at –196 °C using NOVA 3200e (Quantachrome, USA) was applied to characterize the BET-surface area and the texture properties, namely total pore volume ( $V_p$ ) and pore diameter ( $D_p$ ), of various investigated solid catalysts.

### 2.3. Characterizations of the reaction products

All melting points were measured on a Gallenkamp melting point apparatus and are uncorrected. The infrared spectra were recorded in KBr disks on a pye Unicam SP 3300 and Shimadzu FTIR 8101 PC infrared spectrophotometers. The NMR spectra were recorded on a Varian Mercury VX-300 NMR spectrometer.  $^1\text{H}$  spectra were run at 300 MHz and  $^{13}\text{C}$  spectra were run at 75.46 MHz in deuterated chloroform ( $\text{CDCl}_3$ ) or dimethyl sulphoxide ( $\text{DMSO}-d_6$ ). Chemical shifts were related to that of the solvent. Mass spectra were recorded on a Shimadzu GCMS-QP 1000 EX mass spectrometer at 70 eV. Elemental analyses (C, H, N, S) were carried out at the Microanalytical Center of Cairo University, Giza, Egypt, the results were found to be in good agreement ( $\pm 0.3\%$ ) with the calculated values. Microwave experiments were carried out using CEM Discover Labmate<sup>TM</sup> microwave apparatus (300 W with ChemDriver<sup>TM</sup> Software).

### 2.4. Typical procedure for the catalyst test reaction

#### 2.4.1. Method A: microwave irradiation

HT-As (0.5 g), was added to an enaminone derivative (**1a** or **1b**) (10 mmol) and one of the 5-amino-1H-pyrazole derivatives (**2a–c**) (10 mmol) in a mortar, the mixture was ground with a pestle at room temperature then placed in an Pyrex tube in the microwave reactor and irradiated for a suitable time (Table 3) with a 2 min interval. The progress of the reaction was monitored by TLC. Upon completion of the reaction, the mixture was cooled and the product was extracted by dissolution in hot alcohol after evaporating the volatile materials by vacuum, compounds **4a–c** were re-crystallized from ethanol. The catalyst used was redeemed by washing with hot alcohol. Compound **4b** was obtained in the presence of various catalysts (such as HT-As, HT-450 and HT-450-H) and also in neat conditions under microwave irradiation. It was found that all catalysts used exhibited catalytic activity but HT-As was the most effective of all the catalysts tested to promote the reaction with high yield in short time (Table 2).

#### 2.4.2. Method B: conventional method

These processes were performed on the same scale described above for method A. Here the reactant and catalyst were put in ethanol under reflux for 5–8 h (Table 4) until the starting materials were no longer detectable by TLC. The products were obtained and purified as described above in method A.

Physical and spectral data of the title compounds **3a–f** are listed below.

**2.4.2.1. 2-Methyl-7-phenylpyrazolo[1,5-a]pyrimidine (3a).** m.p. 125 °C [lit. [43] m.p. 123–125 °C], IR (KBr)  $\nu_{\text{max}}/\text{cm}^{-1}$ : 1599 (C=N);  $^1\text{H}$  NMR ( $\text{CDCl}_3$ ):  $\delta$  2.29 (s, 3H,  $\text{CH}_3$ ), 6.28 (s, 1H, H-3), 6.96 (d, 2H,  $J=4.2$  Hz, H-6), 6.99–8.01 (m, 5H, Ar-H), 8.33 (d,  $J=4.2$  Hz, 2H, H-5).  $^{13}\text{C}$  NMR ( $\text{CDCl}_3$ ):  $\delta$  13.71, 92.79, 115.09, 127.54, 128.49, 128.89, 133.45, 143.08, 146.11, 151.34, 157.44; MS ( $m/z$ ): 209( $\text{M}^+$ ).

**2.4.2.2. 2,7-Diphenylpyrazolo[1,5-a]pyrimidine (3b).** m.p. 157 °C [lit. [43] m.p. 157 °C], IR (KBr)  $\nu_{\text{max}}/\text{cm}^{-1}$ : 1601 (C=N);  $^1\text{H}$  NMR ( $\text{CDCl}_3$ ):  $\delta$  6.92 (d,  $J=5.1$  Hz, 2H, H-6), 6.99 (s, 1H, H-3), 7.42–8.24 (m, 10H, Ar-H), 8.45 (d,  $J=5.1$  Hz, 2H, H-5).  $^{13}\text{C}$  NMR ( $\text{CDCl}_3$ ):  $\delta$  91.59, 116.84, 126.45, 126.67, 128.88, 128.94, 129.88, 130.78, 132.00, 132.02, 145.78, 148.15, 151.44, 156.21; MS ( $m/z$ ): 271( $\text{M}^+$ ).

**2.4.2.3. 2-(4-Methoxyphenyl)-7-phenylpyrazolo[1,5-a]pyrimidine (3c).** m.p. 172 °C, IR (KBr)  $\nu_{\text{max}}/\text{cm}^{-1}$ : 1598 (C=N);  $^1\text{H}$  NMR ( $\text{CDCl}_3$ ):  $\delta$  3.61 (s, 3H,  $\text{OCH}_3$ ), 6.59 (s, 1H, H-3), 7.01 (d,  $J=4.2$  Hz, 2H, H-6), 7.38–8.01 (m, 9H, Ar-H), 8.33 (d,  $J=4.2$  Hz, 2H, H-5).  $^{13}\text{C}$  NMR ( $\text{CDCl}_3$ ):  $\delta$  52.80, 95.02, 113.26, 116.84, 126.02, 126.59,

127.94, 129.41, 131.98, 136.59, 146.85, 148.09, 151.49, 155.29, 159.42; MS ( $m/z$ ): 301( $\text{M}^+$ ).

**2.4.2.4. 2-Methyl-7-(4-fluorophenyl)pyrazolo[1,5-a]pyrimidine (3d).** m.p. 135–137 °C, IR (KBr)  $\nu_{\text{max}}/\text{cm}^{-1}$ : 1601 (C=N);  $^1\text{H}$  NMR ( $\text{CDCl}_3$ ):  $\delta$  2.08 (s, 3H,  $\text{CH}_3$ ), 6.12 (s, 1H, H-3), 6.89 (d, 2H,  $J=4.8$  Hz, H-6), 7.14–7.78 (m, 4H, Ar-H), 8.20 (d,  $J=4.8$  Hz, 2H, H-5).  $^{13}\text{C}$  NMR ( $\text{CDCl}_3$ ):  $\delta$  13.11, 92.54, 116.19, 118.23, 118.24, 127.50, 128.18, 128.19, 142.54, 144.17, 148.00, 152.45, 161.12; MS ( $m/z$ ): 227( $\text{M}^+$ ).

**2.4.2.5. 7-(4-Fluorophenyl)-2-phenylpyrazolo[1,5-a]pyrimidine (3e).** m.p. 169 °C, IR (KBr)  $\nu_{\text{max}}/\text{cm}^{-1}$ : 1605 (C=N);  $^1\text{H}$  NMR ( $\text{CDCl}_3$ ):  $\delta$  6.39 (d,  $J=4.2$  Hz, 2H, H-6), 6.99 (s, 1H, H-3), 7.10–8.13 (m, 9H, Ar-H), 8.51 (d,  $J=4.2$  Hz, 2H, H-5).  $^{13}\text{C}$  NMR ( $\text{CDCl}_3$ ):  $\delta$  90.52, 116.22, 118.84, 125.62, 125.65, 128.88, 128.94, 129.87, 129.88, 130.14, 130.15, 134.19, 142.62, 144.89, 148.78, 151.44, 161.62; MS ( $m/z$ ): 289( $\text{M}^+$ ).

**2.4.2.6. 7-(4-Fluorophenyl)-2-(4-methoxyphenyl)pyrazolo[1,5-a]pyrimidine (3f).** m.p. 186–188 °C, IR (KBr)  $\nu_{\text{max}}/\text{cm}^{-1}$ : 1601 (C=N);  $^1\text{H}$  NMR ( $\text{CDCl}_3$ ):  $\delta$  3.89 (s, 3H,  $\text{OCH}_3$ ), 6.95 (s, 1H, H-3), 7.16 (d,  $J=4.5$  Hz, 2H, H-6), 7.25–8.13 (m, 8H, Ar-H), 8.26 (d,  $J=4.5$  Hz, 2H, H-5).  $^{13}\text{C}$  NMR ( $\text{CDCl}_3$ ):  $\delta$  54.12, 90.12, 113.11, 116.12, 118.15, 118.6, 123.24, 126.00, 128.99, 129.00, 131.98, 142.58, 144.45, 148.98, 151.11, 160.01, 161.59; MS ( $m/z$ ): 319( $\text{M}^+$ ).

## 3. Results and discussion

### 3.1. Catalyst characterization

#### 3.1.1. Elemental chemical analysis (ICP)

ICP analysis of HT-As was performed to determine its chemical composition. The analysis revealed that the Mg/Al molar ratio was 1.8, which is very close to the nominal molar composition of the pre-calculated Mg/Al molar ratio of 2. This result confirmed the effectiveness of the precipitation process.

#### 3.1.2. X-ray diffraction (XRD)

X-ray powder diffraction patterns of as-synthesized hydrotalcite (HT-As) are shown in Fig. 2. A phase analysis shows that only a hydrotalcite layered structure is obtained (Ref. Pattern 22-0700, JCPDS) with sharp and intense peaks for the (003), (006), (009), (110) and (113) planes and broad peak for the (015) plane. The crystal structure of the investigated HT-As was rhombohedral with  $R\bar{3}m$  space group. The lattice parameters were calculated and the average crystallite sizes were estimated from the Scherrer equation using the FWHM of the basal reflection plane (003) and the non basal line (110). The calculated lattice parameter  $a$ , which is mainly related to the cation composition, was equal to 0.306 nm. The  $a$  value decreases as the Al content increases from the initial value of the Al-free brucite phase to the synthesized Mg/Al-hydrotalcite [47]. The calculated cell parameter  $c$ , which is directly linked to the interlayer distance, was equal to 2.34 nm, and the obtained crystallite size was 19 nm. The longer dimension in the  $c$  direction is mainly attributed to the relatively large distance between cation sheets of hydrotalcites. The calcination of as-synthesized hydrotalcite phase at 450 °C (HT-450) led to the formation of an amorphous magnesium oxide phase (periclase: Ref. Pattern 45-0946, JCPDS) [48,49].

The liquid phase hydration of calcined hydrotalcite at 450 °C (HT-450-H) did not fully match that of the initial hydrotalcite (HT-As). The method of hydration of calcined hydrotalcite phase affects the re-hydrated phase structure. The phase formed after liquid water hydration of the calcined solid at 450 °C is a hydrotalcite-like phase named meixnerite [49]. These changes in the phase structure

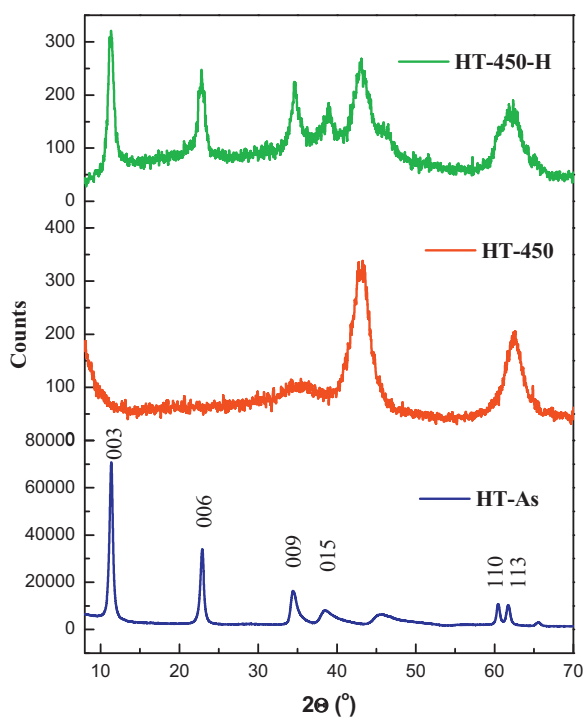


Fig. 2. XRD patterns of hydrotalcite and activated hydrotalcite samples.

and pattern intensities affect the texture and catalytic properties of the investigated catalysts.

### 3.1.3. Fourier transform infrared spectroscopy (FTIR)

FTIR spectra of HT-As sample (Fig. 3) showed a broad band at  $3484\text{ cm}^{-1}$  assigned to the O–H stretching vibration, which is ascribed to interlayer water and hydroxyl groups in hydroxide layer

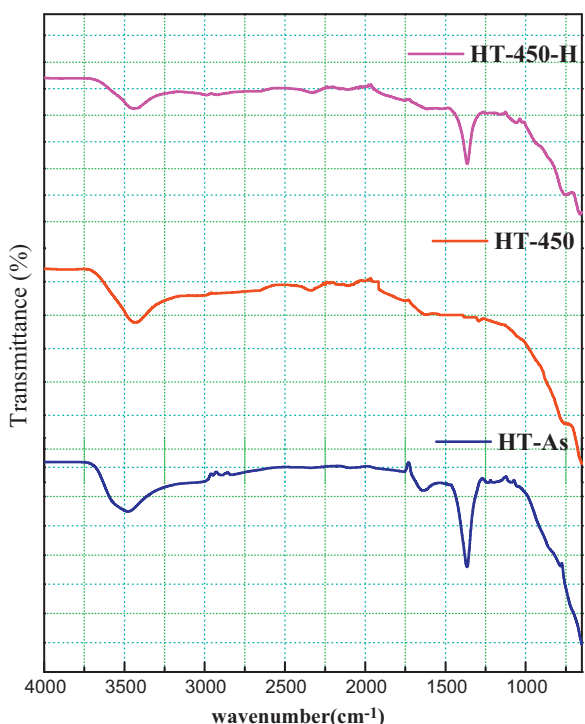


Fig. 3. FTIR spectra of hydrotalcite and activated hydrotalcite samples.

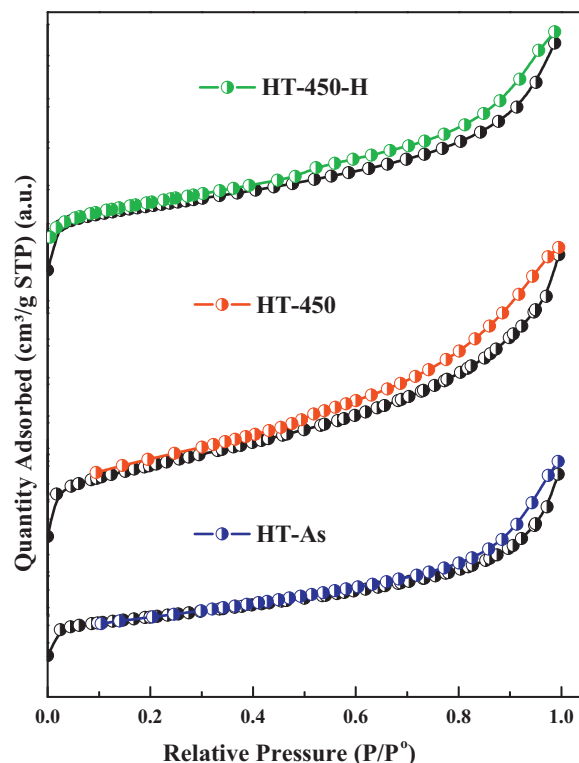
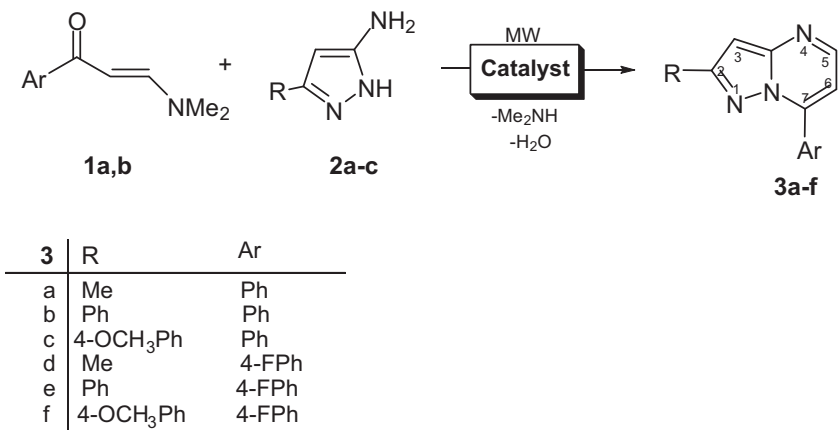


Fig. 4. Adsorption/desorption isotherms of hydrotalcite and activated hydrotalcite samples.

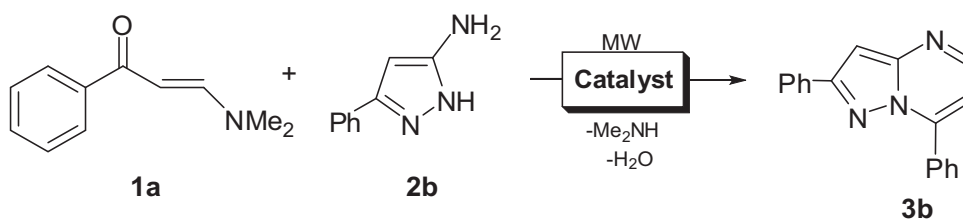
of hydrotalcite [50], thus distinct from water adsorbed on clay minerals where the OH-stretching modes of weak hydrogen bonds occur in the region between  $3600$  and  $3500\text{ cm}^{-1}$ . The shoulder at  $2809\text{ cm}^{-1}$  is assigned to hydroxyl interactions with carbonate ions in the interlayer – more specifically it has been attributed to the bridging mode  $\text{H}_2\text{O}-\text{CO}_3^{-2}$ . A weak peak around  $1630\text{ cm}^{-1}$  in the infrared spectrum is attributed to the  $\nu\text{ H}_2\text{O}$  mode of water in the interlayer. The high vibration frequency is attributed to symmetry restrictions induced by the hydrogen bonded carbonate ions to hydroxyl groups of the hydroxide sheets. The peak around  $1360\text{ cm}^{-1}$  related to  $\nu_3$  band of carbonate [51]. The carbonate band of as-synthesized hydrotalcite was vanished completely upon calcinations at  $450^\circ\text{C}$  (HT-450). This is attributed to the complete thermal decomposition of hydrotalcite phase into mixed metal oxides, which complements the XRD data. However, the hydration of the calcined phase (HT-450-H) led to the formation of hydroxyl and carbonate groups in the interlayer gallery of activated oxide.

### 3.1.4. $\text{N}_2$ -physisorption

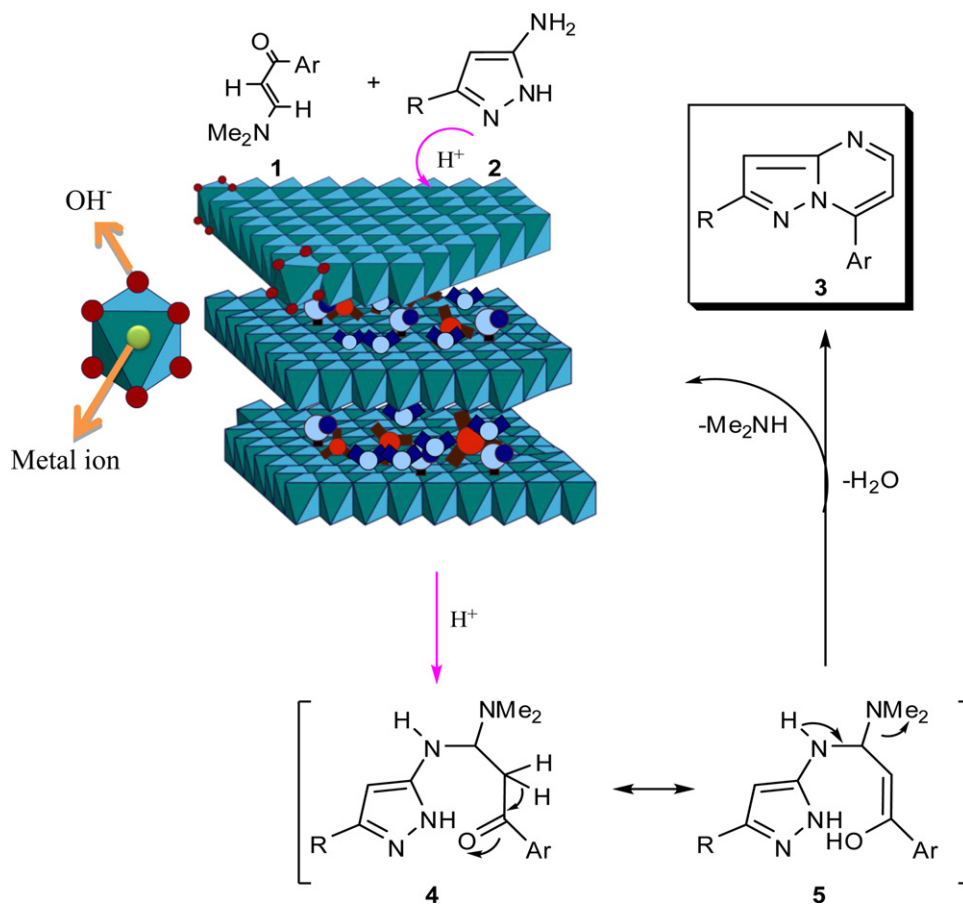
Fig. 4 represents the  $\text{N}_2$  adsorption/desorption isotherms of all the investigated samples. Type IV sorption isotherm with H3-type hysteresis at relatively high relative pressure is displayed for all samples. The isotherm exhibits an H3-type hysteresis at high relative pressure, which is typical for aggregates of plate-like particles [52]. The enclosure of adsorption/desorption branches at relatively high  $p/p^0 = 0.7$ , for HT-As sample, could be attributed to the presence of large mesoporous structure and/or some macropores. This kind of hysteresis is typical for the presence of open large pores, which allow easy diffusion of the reactants through the materials. On contrary to that, both HT-450 and HT-450-H samples show an enclosure of adsorption/desorption branches at relatively low  $p/p^0 = 0.4$ . The fast increase in the amount of adsorbed nitrogen in the range of very low relative pressures is an indication of the presence of some microporosity. The specific surface area of HT-As showed the smallest surface area of all the investigated solids,



**Scheme 1.** Synthesis of pyrazolo[1,5-*a*]pyrimidine derivatives **3a–f**.



**Scheme 2.** Synthesis of 2,7-diphenylpyrazolo[1,5-*a*]pyrimidine (**3b**) in absence and in presence of different catalysts under microwave irradiation.



**Scheme 3.** Suggested mechanism for the catalytic synthesis of pyrazolo[1,5-*a*]pyrimidines using MgAl-HT catalysts.

**Table 1**

Texture properties of different samples obtained from N<sub>2</sub> adsorption/desorption isotherms.

Sample	S <sub>BET</sub> (m <sup>2</sup> /g)	V <sub>p</sub> (cm <sup>3</sup> /g)	r <sub>p</sub> (Å)	C-constant
HT-As	86.26	0.1742	40.41	184.5
HT-450	171.26	0.2854	33.33	82.70
HT-450-H	138.59	0.2146	30.97	579.8

**Table 2**

Reaction of **1a** with **2b** in absence and in presence of different catalysts carried out under microwave irradiations.

Catalyst	Reaction time <sup>a</sup> (min)	Yield %
Blank experiment	No reaction	–
HT-As	18	94
HT-450	44	70
HT-450-H	42	75

<sup>a</sup> Reaction conditions: solvent-free condition, 10 mmol of enaminone derivative and 10 mmol of aminopyrazole derivative, 0.5 g of catalyst under microwave irradiations.

while the thermal treatment of hydrotalcite at 450 °C resulted in a pronounced increase in the specific surface area (Table 1). Such a behavior has been reported for hydrotalcites containing carbonates and assigned to the formation of craters through the layers due to evolution of CO<sub>2</sub> and H<sub>2</sub>O [53]. Hydration of the calcined hydrotalcite in the liquid phase by mechanical stirring resulted in an increase in surface area due to the rupture of particles and a marked exfoliation of the crystals [54].

### 3.2. Catalytic activity study

The catalytic activity of the as-synthesized and activated hydrotalcites towards the aza-Michael addition reaction (Scheme 1) was evaluated. Thus, the reaction of an enaminone (**1a,b**) with the 5-amino-1*H*-pyrazole derivatives (**2a–c**) in the presence hydrotalcite catalysts was carried out without solvent under microwave irradiation, to obtain only one isolable product in each case, (as examined by TLC) which were identified as pyrazolo[1,5-*a*]pyrimidine derivatives **3a–f** (Scheme 1).

All the isolated products **3a–f** gave satisfactory elemental analyses and the obtained spectroscopic data (IR, <sup>1</sup>H NMR, <sup>13</sup>C NMR, MS) was consistent with their assigned structures. The IR spectra of the products showed the absence of carbonyl absorption band and amino group absorption bands. The mass spectra of the isolated products, such as **3c**, showed a peak corresponding to the molecular ion at *m/z* 301 (see characterization of the reaction products). Its <sup>1</sup>H NMR spectrum revealed a singlet signal at δ 3.61(OCH<sub>3</sub>), a singlet signal at δ 6.59(CH-3) and two doublet signals at δ 7.01, 8.33 (*J* = 5.1 Hz) due to pyrimidine protons (CH-6, CH-5), respectively, in addition to aromatic protons as a multiplet at δ 7.38–8.01.

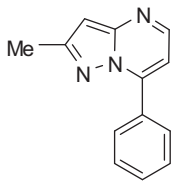
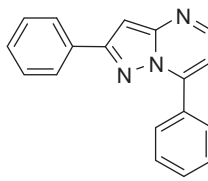
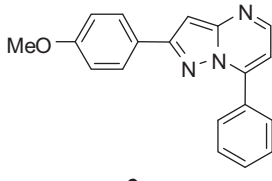
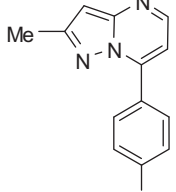
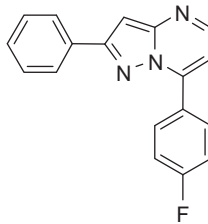
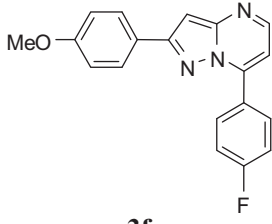
To find optimum conditions for the microwave assisted solvent free reaction of **1a,b** with **2a–c** using the as-synthesized and activated hydrotalcites, the reaction of **1a** with **2b**, in absence and/or presence of different hydrotalcite catalysts, was selected as a model reaction (Scheme 2).

The results obtained from the catalytic test reaction are cited in Table 2. In blank experiments (without a catalyst), no product formation was observed.

We performed catalytic studies of HT-As and activated samples by monitoring product formation; the activities of the catalysts different significantly (Table 2). The target product was formed with 100% conversion. It is shown from this table that using the hydrotalcite and activated hydrotalcites as catalysts resulted in acceptable yields of the products. The as-prepared hydrotalcite (HT-As) is the most effective catalyst for the synthesis of

**Table 3**

The efficiency of HT-As catalyst towards the synthesis of different pyrazolo[1,5-*a*]pyrimidine derivatives **3a–f**.

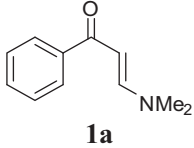
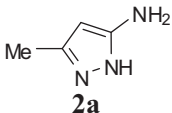
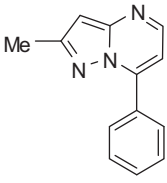
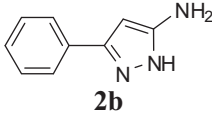
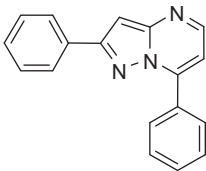
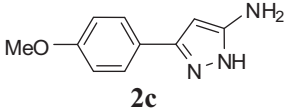
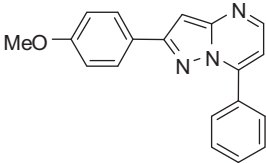
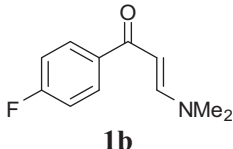
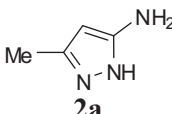
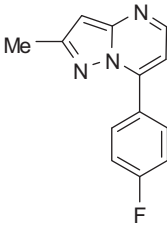
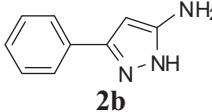
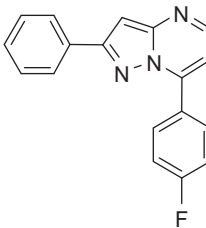
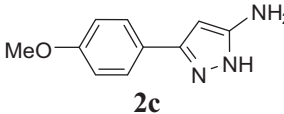
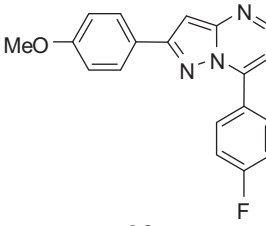
Compound no.	Reaction time <sup>a</sup> (min)	Yield	Lit. yield <sup>**</sup>
 <b>3a</b>	15	93%	64% [43]
 <b>3b</b>	18	92%	53% [43]
 <b>3c</b>	18	92%	–
 <b>3d</b>	15	92%	–
 <b>3e</b>	16	90%	–
 <b>3f</b>	15	90%	–

<sup>a</sup> Reaction conditions: solvent-free condition, 10 mmol of enaminone derivatives and 10 mmol of aminopyrazole derivatives, 0.5 g of HT-As catalyst under microwave irradiations.

<sup>\*\*</sup> Lit. conditions [43]: Reflux in ethanol/piperidine.

pyrazolo[1,5-*a*]pyrimidine derivative **3b**, since the highest yield was achieved in a shortest time. Therefore, this particular catalyst was selected as the best catalyst to test the other reactions and the results are summarized in Table 3. It is seen from Table 3 that HT-As catalyst shows an efficient activity and higher % yield in comparison

**Table 4**  
Synthesis of pyrazolo[1,5-*a*]pyrimidine **3a–f** under conventional method using HT-As catalyst.

Enaminone	Heterocyclic Amines	Products	Reaction time* (h)	Yield (%)
			5	79
			5	74
			6	76
			5	81
			6	77
			6	75

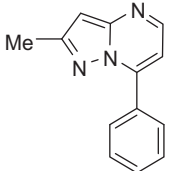
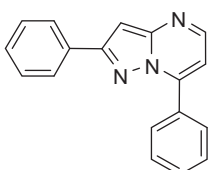
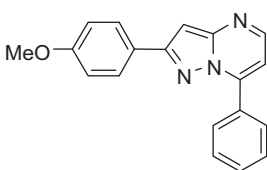
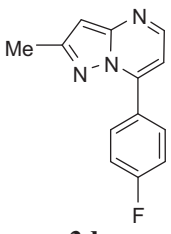
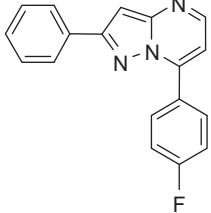
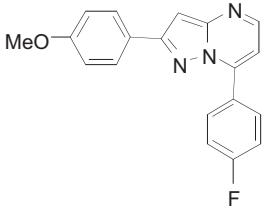
\* Reaction conditions: 10 mmol of enaminone derivative and 10 mmol of aminopyrazole derivative, 0.5 g of HT-As under reflux in ethanol.

to the literature data. Moreover, some new organic compounds were synthesized using HT-As catalyst in short time (15–18 min) and acceptable % yield.

The catalytic performance of HT-As, HT-450, and HT-450-H for aza-Michael addition reaction depends on their acidic/basic site nature. Calcinations of as-synthesized hydrotalcites often create more Lewis basic sites [54]. Moreover, the hydration of the calcined hydrotalcite sample usually gives hydrated phases with high

number of Brønsted basic sites [54]. Hence, one may conclude that Brønsted basic hydroxyl groups are not alone sufficient, while contributions of Lewis acidic sites ( $Al^{3+}$ ) might not be ruled out for driving this reaction [55]. The location of  $Al^{3+}$  cation in the cationic sheet is greatly affected by the calcination temperature and rehydration process [56–59]. In our recent publication we have claimed that the high propensity of trivalent Al-ions to migrate to tetrahedrally coordinated lattice sites upon calcination and rehydration

**Table 5**  
The durability test of the HT-As catalyst towards the synthesis of pyrazolo[1,5-*a*]pyrimidine derivative **3a–f**.

Compound no.	Number of successive uses of HT-As catalyst/yield (%)				
	1st	2nd	3rd	4th	5th
<i>Time to reach 100% conversion (min)</i>					
 <b>3a</b>	15/93	15/93	15/93	15/90	15/88
 <b>3b</b>	18/92	18/92	18/91	18/88	20/86
 <b>3c</b>	18/92	18/92	18/90	18/87	21/86
 <b>3d</b>	15/92	15/92	15/91	15/90	16/89
 <b>3e</b>	15/90	15/90	15/89	15/88	18/86
 <b>3f</b>	15/90	15/90	16/89	16/89	18/88

process [60]. Such changes in cation location affect the role of  $\text{Al}^{3+}$  cation from the as-synthesized hydrotalcite (HT-As) to the activated samples. Therefore, the pronounced efficiency of the as-synthesized catalyst, over the activated ones, could be attributed to the different roles played by  $\text{Al}^{3+}$  cation together with the Brønsted basic sites of this particular catalyst, which acts as a bi-functional catalyst [55]. Such bi-functionality is of use for reactions such as the

aza-Michael addition reaction since it can be carried out in acidic or basic conditions.

These results encourage us to suggest a mechanism of the reaction in which, to our knowledge, no established mechanism for the formation of pyrazolo[1,5-*a*]pyrimidines using hydrotalcite as a catalyst has been reported. A plausible mechanism is shown in Scheme 3.

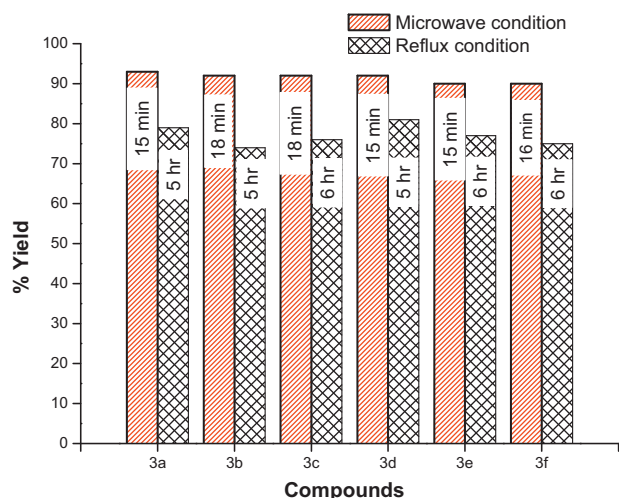


Fig. 5. Catalytic performance of HT-As under conventional and microwave conditions: time to accomplish the reaction is given in graph bars.

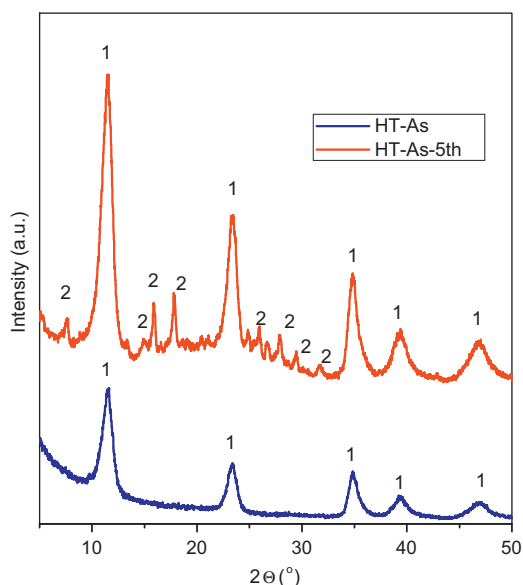


Fig. 6. XRD patterns of HT-As and HT-As catalyst after 5th time working conditions. (1) Hydrotalcite phase and (2) organic contaminants.

It is presumed that the reaction proceeds *via* adsorption of educts lone pair donation to the acidic sites ( $\text{Al}^{3+}$ ), while the Brønsted basic sites ( $\text{OH}^-$ ) of the hydrotalcite facilitates the nucleophilic addition *via* deprotonation/re-protonation process resulting in the Michael addition adduct **4**. A subsequent cyclization *via* dehydration then aromatization *via* loss of dimethyl amine molecule produces the pyrazolo[1,5-*a*]pyrimidine derivatives.

In order to address for the advantage of microwave irradiation on this reaction, the previously mentioned reaction were carried out using conventional method using hydrotalcite catalysts in ethanol as solvent (Table 4). The obtained results revealed that the reactions are carried out in a longer time to attain a much lower yield than that obtained using microwave protocol.

The results of the screening experiments for this reaction (under both microwave and reflux condition), which were carried out using the HT-As sample, are presented in Fig. 5.

The reactions carried out under microwave irradiation show better yield in very short time relative to the classical preparation method (Fig. 5). The microwave shows a beneficial effect on the synthesis of pyrazolo[1,5-*a*]pyrimidine derivatives, in which, a decrease in time of the above reactions from 6 h in conventional procedure to around 20 min was occurred.

It was necessary to study the durability of the HT-As catalyst in the microwave assisted reactions. Therefore, each reaction was repeated five times using a regenerated catalyst. The MgAl-hydrotalcite (HT-As) catalyst was removed after the reaction by filtration, washed with ethanol and dried under *vacuo*. The recovered catalyst is reused several times and the time required to accomplish the reaction was taken as an indication of catalytic activity, and the results obtained are given in Table 5.

Table 5 shows that the regenerated catalyst performs the reactions efficiently under constant reaction conditions even after being used for 5 times. The slight decay observed in the catalytic activity of the HT-As catalyst on the 5th time of being used could be attributed to temporary poisoning by organic contaminants and/or to the change in the crystal structure of the catalyst under the operating conditions. To confirm these speculations the catalyst that had been reused 5 times under microwave irradiation conditions were characterized using XRD.

It is shown in Fig. 6 that the intensity of the XRD patterns increases after 5th time of being subjected to the irradiations from the microwave during the reaction, which is indicative of an increase in the degree of crystallinity of the hydrotalcite phase. The undefined patterns are believed to relate to some organic contaminants that are presumed to cause some temporary poisoning of the catalyst. These results explain the minor decay of the HT-As catalyst after repeated re-use under these operating conditions.

#### 4. Conclusions

An efficient benign method for the synthesis of pyrazolo[1,5-*a*]pyrimidine derivatives using a MgAl-hydrotalcite catalyst, under microwave irradiation has been established. A significantly higher yield and shorter reaction time was observed when using the as-synthesized Mg–Al-hydrotalcite rather than the other activated HT catalysts. The pronounced catalytic performance of the as-synthesized Mg–Al-hydrotalcite is mainly due to appropriate cooperative behavior of acid–base pair sites. A suggested mechanism for aza-Michael addition reaction has been provided using an as-synthesized Mg–Al-hydrotalcite bi-functional acid–base catalyst for the first time. The prepared catalyst showed constant durability until the 5th time of reuse under the specific operating conditions.

#### Acknowledgements

This work was supported by the deanship of scientific research at King Abdulaziz University and Saudi Basic Industries Corporation (SABIC) (project no. MS 3/11). The Authors are grateful to Dr Felicity Sartain for her contribution to discussions and assistance during this research.

#### References

- [1] E. Angelescu, O.D. Pavel, R. Bîrjega, R. Zăvoianu, G. Costentin, M. Che, Appl. Catal. A: Gen. 308 (2006) 13.
- [2] W. Reichle, J. Catal. 63 (1980) 295.
- [3] A. Corma, R.M. Martín-Aranda, Appl. Catal. A: Gen. 105 (1993) 271.
- [4] A. Corma, V. Fornes, F. Rey, J. Catal. 148 (1994) 205.
- [5] J.I. Di Cosimo, V.K. Díez, M. Xu, E. Iglesia, C.R. Apesteguía, J. Catal. 178 (1998) 499.
- [6] G.J. Kelly, F. King, M. Kett, Green Chem. 4 (2002) 392.

- [7] J.C.A.A. Roelofs, D.J. Lensveld, A.J. van Dillen, K.P. de Jong, *J. Catal.* 203 (2001) 184.
- [8] F. Figueras, J. Lopez, J. Sanchez-Valente, T.T.H. Vu, J.M. Clacens, J. Palomeque, *J. Catal.* 211 (2002) 144.
- [9] D. Carriazo, C. Martin, V. Rives, A. Popescu, B. Cojocar, I. Mandache, V.I. Parvulescu, *Micropor. Mesopor. Mater.* 95 (2006) 39.
- [10] J.S. Valente, F. Figueras, M. Gravelle, J. Lopez, J.-P. Besse, *J. Catal.* 189 (2000) 370.
- [11] V.K. Srivastava, H.C. Bajaj, R.V. Jasra, *Catal. Commun.* 4 (2003) 543.
- [12] D. Tichit, B. Coq, S. Cerneaux, R. Durand, *Catal. Today* 75 (2002) 197.
- [13] M.J. Climent, A. Corma, S. Iborra, J. Primo, *J. Catal.* 151 (1995) 60.
- [14] D. Tichit, M.N. Bennani, F. Figueras, R. Tessier, J. Kervenal, *Appl. Clay Sci.* 13 (1998) 401.
- [15] D. Tichit, D. Latic, B. Coq, R. Durand, R. Teissier, *J. Catal.* 219 (2003) 167.
- [16] S.K. Sharma, P.A. Parikh, R.V. Jasra, *J. Mol. Catal. A: Chem.* 286 (2008) 55.
- [17] J.-A. Ma, H.-C. Guo, *Angew. Chem. Int. Ed.* 45 (2006) 354.
- [18] M.R. Shaaban, T.S. Saleh, A.M. Farag, *Heterocycle* 71 (2007) 1765.
- [19] A.A. Elassar, A.A. El-Khair, *Tetrahedron* 59 (2003) 8463.
- [20] K.M. Alzaydi, *Molecules* 8 (2003) 541.
- [21] S. Kobayashi, K. Kakumoto, M. Sugiura, *Org. Lett.* 4 (2002) 1319.
- [22] L.-W. Xu, J.W. Li, C.-G. Xia, S.-L. Zhou, X.-X. Hu, *Synlett* (2003) 2425.
- [23] T.P. Loh, L.L. Wei, *Synlett* (1998) 975.
- [24] S. Matsubara, M. Yoshiyoka, K. Utimoto, *Chem. Lett.* (1994) 827.
- [25] G. Jenner, *Tetrahedron Lett.* 36 (1995) 233.
- [26] N. Azizi, M.R. Said, *Tetrahedron* 60 (2004) 383.
- [27] N. Srivastava, B.K. Banik, *J. Org. Chem.* 68 (2003) 2109.
- [28] L.-W. Xu, L. Li, C.-G. Xia, *Helv. Chim. Acta* 87 (2004) 1522.
- [29] G. Bartoli, M. Bosco, E. Marcantoni, M. Petrini, L. Sanbri, E. Torregiani, *J. Org. Chem.* 66 (2001) 9052.
- [30] A. Zare, A. Hasaninejad, A. Khalafi-Nezhad, A.R.M. Zare, A. Parhami, G.R. Nejabat, *Arkivoc* (2007) 58.
- [31] M.J. Bhanushali, N.S. Nandurkar, S.R. Jagtap, B.M. Bhanage, *Catal. Commun.* 9 (2008) 1189.
- [32] C. Mukherjee, A.K. Misra, *Lett. Org. Chem.* 4 (2007) 5458.
- [33] B.M. Reddy, M.K. Patil, B.T. Reddy, *Catal. Lett.* 126 (2008) 413.
- [34] M.L. Kantam, B. Neelima, C.V. Reddy, *J. Mol. Catal. A: Chem.* 241 (2005) 147.
- [35] H.A. Abdel-Aziz, T.S. Saleh, H.S.A. El-Zahabi, *Arch. Pharm. Chem. Life Sci.* 343 (2010) 24.
- [36] M.S.A. El-Gaby, A.A. Atalla, A.M. Gaber, K.A. Abd Al-Wahab, *Farmaco* 55 (2000) 596.
- [37] S. Sella, F. Bruni, C. Costagli, A. Costanzo, G. Guerrini, G. Ciciani, B. Costa, C. Martini, *Bioorg. Med. Chem.* 7 (1999) 2705.
- [38] I. Makoto, O. Takashi, S. Yasuo, H. Kinji, O. Masayuki, Y. Sunee, US Patent 98,43,951 (1998).
- [39] J. Hedner, R. Yaeche, G. Emilien, I. Farr, E. Salinas, *Int. J. Geriatr. Psychiatry* 15 (2000) 704.
- [40] C. Chen, K.M. Wilcoxon, C.Q. Huang, J.R. McCarthy, T. Chen, D.E. Grigoriadis, *Bioorg. Med. Chem. Lett.* 14 (2004) 3669.
- [41] M. Mokhtar, T.S. Saleh, N.S. Ahmed, S.A. Al-Thabaiti, R.A. Al-Shareef, *Ultrason. Sonochem.* 18 (2011) 172.
- [42] T.S. Saleh, N.M. Abd El-Rahman, *Ultrason. Sonochem.* 16 (2009) 237.
- [43] A. Al-Enezi, B. Al-Saleh, M.H. El-Nagdi, *J. Chem. Res. (S)* (1997) 4, (M) (1997) 116.
- [44] S. Kantevari, M.V. Chary, S.V.N. Vuppapapati, *Tetrahedron* 63 (2007) 13024.
- [45] M. Takamizawa, Y. Hamashima, *Yakugaky zasshi* 84 (1964) 1113.
- [46] F. Cavani, F. Trifiro, A. Vaccari, *Catal. Today* 11 (1991) 173.
- [47] V.K. Díez, C.R. Apesteguía, J.I. Di Cosimo, *J. Catal.* 215 (2003) 220.
- [48] J. Pérez-Ramírez, S. Abelló, N.M. Van der Pers, *J. Phys. Chem. C* 111 (2007) 3642.
- [49] M. Mokhtar, A. Inayat, J. Ofili, W. Schwiager, *Appl. Clay Sci.* 50 (2010) 176.
- [50] D.P. Das, J. Das, K. Parida, *J. Colloid Inter. Sci.* 261 (2003) 213.
- [51] K. Pil, K. Younghun, K. Heesoo, K.S. In, Y. Jongheop, *Appl. Catal. A: Gen.* 272 (2004) 157.
- [52] D. Meloni, R. Monaci, V. Solinas, A. Auroux, E. Dumitriu, *Appl. Catal. A: Gen.* 350 (2008) 86.
- [53] W.T. Reichle, S.Y. Kang, D.S. Everhardt, *J. Catal.* 101 (1986) 352.
- [54] S. Abelló, F. Medina, D. Tichit, J. Pérez-Ramírez, J.E. Sueiras, P. Salagre, Y. Cesteros, *Appl. Catal. B: Environ.* 70 (2007) 577.
- [55] C.A. Antonyraj, S. Kannan, *Appl. Catal. A: Gen.* 338 (2008) 121.
- [56] D. Tichit, M.N. Bennani, F. Figueras, J.R. Ruiz, *Langmuir* 14 (1998) 2086.
- [57] M. Bellotto, B. Rebours, O. Clause, J. Lynch, D. Bazin, E. Elkaïm, *J. Phys. Chem.* 100 (1996) 8535.
- [58] J. Rocha, M. del Arco, V. Rives, M.A. Ulibarri, *J. Mater. Chem.* 9 (1999) 2499.
- [59] J.C.A.A. Roelofs, J.A. van Bokhoven, A.J. van Dillen, J.W. Geus, K.P. de Jong, *Chem. Eur. J.* 8 (2002) 5571.
- [60] M.C.D. Mourad, M. Mokhtar, M.G. Tucker, E.R. Barney, R.I. Smith, A.O. Alyoubi, S.N. Basahel, M.S.P. Shaffer, N.T. Skipper, *J. Mater. Chem.* 21 (2011) 15479.